Bioinsp. Biomim. 1 (2006) L1–L6 doi:10.1088/1748-3182/1/3/L01

COMMUNICATION

Thriving at high hydrostatic pressure: the example of ammonoids (extinct cephalopods)

Fabio Vittorio De Blasio

Department of Geosciences, University of Oslo, Box 1047 Blindern, 0316 Oslo, Norway

E-mail: fvb@ngi.no

Received 26 May 2006
Accepted for publication 11 September 2006
Published 28 September 2006
Online at stacks.iop.org/BB/1/L1

Abstract

Ammonoids are a group of extinct mollusks belonging to the same class of the living genus *Nautilus* (cephalopoda). In both Nautili and ammonoids, the (usually planospiral) shell is divided into chambers separated by septa that, during their lifetime, are filled with gas at atmospheric pressure. The intersection of septa with the external shell generates a curve called the suture line, which in living and most fossil Nautili is fairly uncomplicated. In contrast, suture lines of ancient ammonoids were gently curved and during the evolution of the group became highly complex, in some cases so extensively frilled as to be considered as fractal curves. Numerous theories have been put forward to explain the complexity of suture ammonoid lines. Calculations presented here lend support to the hypothesis that complex suture lines aided in counteracting the effect of the external water pressure. Additionally, it is suggested that complex suture lines diminished shell shrinkage caused by water pressure, and thus aided in improving buoyancy. Understanding the reason for complex sutures in ammonoids represents an important issue in paleobiology with potential applications to the problem of the resistance of hollow mechanical structures subjected to high pressure.

Introduction

In the marine living mollusk *Nautilus*, a number of internal consecutive septa divide a large part of the shell (called the phragmocone) into chambers filled with gas at atmospheric pressure. This configuration is neutrally or slightly negatively buoyant so that the mollusk floats weightlessly, and a water jet from a conduit (hyponome) is sufficient to propel it horizontally or vertically in the water column. The intersection of septa with the external wall, the so-called suture line, is only slightly curved in most living or fossil Nautili. In contrast, this line features greater complexity in ammonoids, the close extinct relatives of Nautili. Whereas suture lines in early ammonoid species are straight or slightly curved, their patterns became extremely complex during the evolution of the group, when highly sinuous and fractal-like features evolved (see e.g. [1, 2]) with fractal dimension in some cases as high as 1.6–1.7 [3]. Figure 1 shows some examples of suture lines observed in specimens of various geologic periods.

Numerous hypotheses have been put forward to explain the complexity of suture lines. The earliest theories were based on the premise that high sinuosity reinforced the shell against hydrostatic pressure perpendicular to the external shell or parallel to the shell [4], preventing the mollusk from the fatal risk of an implosion when diving in deep waters. Explanations based on the external pressure were further elaborated with possible variants in more recent works [5]. Alternatively, complexity in septa has been regarded as completely unrelated to external pressure. Some researchers have suggested that complex lines increased the attachment area for muscles [6]. Others have envisaged complexity either as a consequence of the morphogenetic processes or as a viscous fingering process [7]. Recently, the pressure hypotheses have been disputed based on the results of finite-element calculations

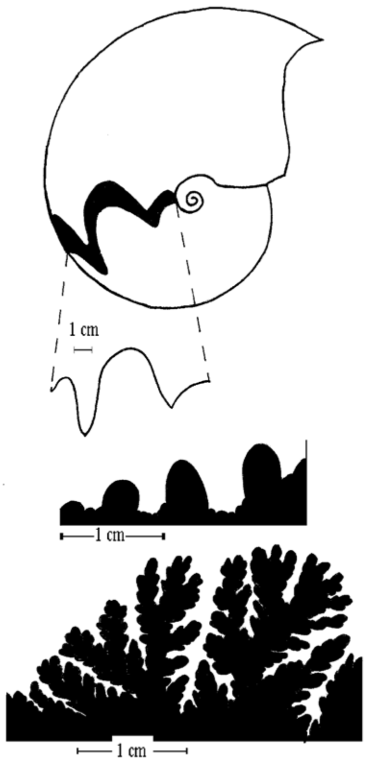

Figure 1. Ammonoid suture lines. Early ammonoids were characterized by slightly sinuous suture lines (termed goniatitic) as in the Devonian genus *Manticoceras* (top). Higher levels of complexity were reached with the ceratitic suture (line in the middle of the figure, *Paraceratites*, Triassic) and then with the ammonitic suture (line at the bottom, *Perisphinctes*, late Jurassic). Only the genus is indicated for each example.

showing that complexity decreases shell resistance [8], though other researchers concluded differently based on comparable modelling techniques [9].

In this communication I present analytical calculations of shell deformation and stress with variable shell complexity. Because of the simplifications made, this work will address only the simplest geometries where suture lines are more or less parallel as in *Manticoceras* (upper drawing in figure 1). Given a certain area of the external shell comprised between two consecutive sutures (the shaded area in figure 1), the ratio of the suture length to the minimum possible length will be used as a proxy for suture complexity [10]. Indeed, it will be argued that the purpose of increasing complexity was to gain a longer septal periphery to buttress the external shell. After showing that the increase in suture length determines a decrease in the stress, I calculate the shrinkage of the shell in response to hydrostatic pressures, showing that shrinkage might have been significant in an ammonoid with a very thin shell and non-complex suture.

Model calculations

A single chamber is modelled as composed of two parallel and flat plates buttressed by two consecutive septa. The external

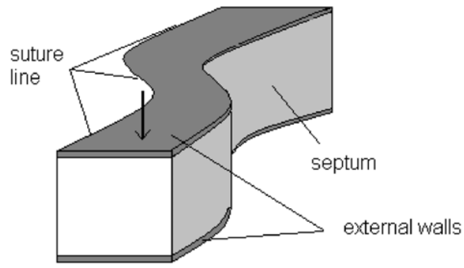

Figure 2. The basic model chamber. The two external walls of each chamber are subjected to water pressure (as indicated by the arrow for the upper wall). The deformation of each external wall is calculated using plate theory.

pressure exerted by water on one chamber will deform the two flat plates inward (figure 2). As a preliminary step, I calculate the displacement of a rectangular plate of sides a and b subjected to an uniform pressure. As a boundary condition, the displacement is set to zero at the margins along the four sides of the plate. The differential equation for plate bending is [11]

$$D\nabla^4 w(x,y) = D\left[\frac{\partial^4 w(x,y)}{\partial x^4} + \frac{\partial^4 w(x,y)}{\partial y^4} + 2\frac{\partial^2 w(x,y)}{\partial x^2}\frac{\partial^2 w(x,y)}{\partial x^2}\right] = P, \qquad (1)$$

where $w(x, y)$ is the displacement of the plate, x and y are the coordinates on the surface of the plate, P is the pressure acting perpendicular to the plate and the flexural rigidity D is given by

$$D = \frac{Eh^3}{12(1-\nu^2)}, \qquad (2)$$

where E is Young's modulus, h is plate thickness and ν is Poisson's parameter. The bending for the rectangular plate can be found with Fourier sinus expansion [11]

$$w(x,y) = \frac{a^4 b^4}{D\pi^4}\sum_{m=1}^{\infty}\sum_{n=1}^{\infty}\frac{q_{mn}}{[m^2b^2+n^2a^2]^2}\sin\left(\frac{m\pi x}{a}\right) \times \sin\left(\frac{n\pi y}{b}\right), \qquad (3)$$

where the Fourier expansion coefficients are given as

$$q_{mn} = 4P\frac{[(-1)^m - 1][(-1)^n - 1]}{mn\pi^2}. \qquad (4)$$

I define the deformation Δ as the volume change of the chamber due to the effect of bending of a single plate (the total volume loss of a chamber is 2Δ owing to the presence of two plates for each chamber). This quantity can be calculated by integration as

$$\Delta = \int_0^a \mathrm{d}x \int_0^b \mathrm{d}y\, w(x,y) = \frac{64}{\pi^8}\frac{a^5b^5P}{D}\sum_{m=0}^{\infty}\sum_{n=0}^{\infty} \times \frac{1}{(2m+1)^2(2n+1)^2[(2m+1)^2b^2+(2n+1)^2a^2]^2}. \qquad (5)$$

The maximum diagonal stresses are reached at the bottom of the plate (namely, inside the phragmocone) and are given as [11]

$$\mathrm{Max}\{\tau_{xx}\} = \frac{6M_x}{h^2}, \qquad \mathrm{Max}\{\tau_{yy}\} = \frac{6M_y}{h^2}, \qquad (6)$$

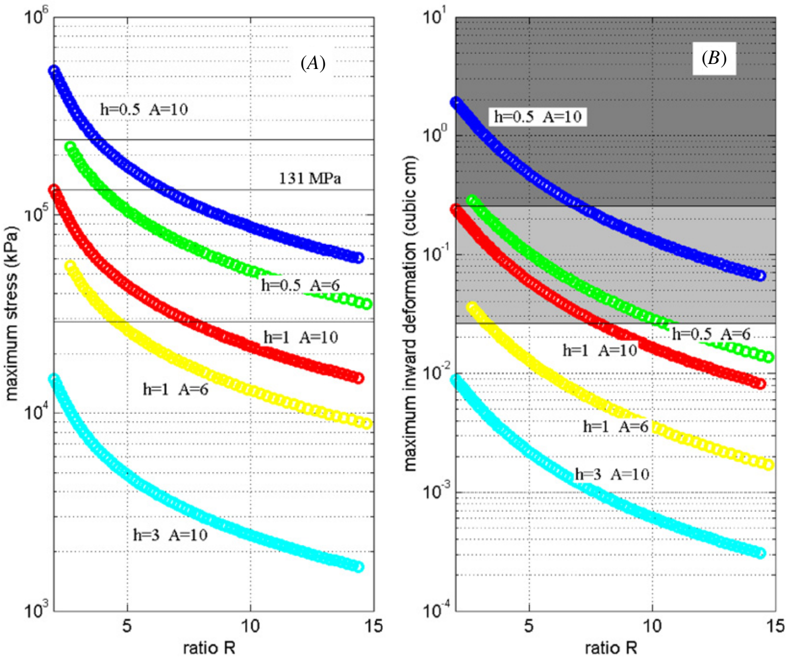

Figure 3. The maximum stress in kPa experienced by one plate (*A*) and shrinkage volume of the plate $\Delta(P = 1 \text{ MPa})$ (*B*, in cm^3) calculated from equation (6) at a pressure of 1 MPa as a function of the ratio $R = a/b$ between the length of the suture line and the distance between successive lines. The parameters for each line are the following (from top to bottom): blue: $h = 0.5$ mm, $A = 10 \text{ cm}^2$; green: $h = 0.5$ mm, $A = 6 \text{ cm}^2$; red: $h = 1$ mm, $A = 10 \text{ cm}^2$; yellow: $h = 1$ mm, $A = 6 \text{ cm}^2$; cyan: $h = 3$ mm, $A = 10 \text{ cm}^2$. The three horizontal lines in the first graph represent three values proposed in the literature for the maximum tensile stress beyond which the shell will break: 29 MPa [4], 131 MPa [5] and 231 MPa [15]. Note that the dependence of the shrinkage volume on the thickness is of the form $\Delta \propto 1/h^3$. The dark shaded area distinguishes the region where the buoyancy loss is higher than the estimation for the thrust force. In the light shaded area, the buoyancy loss is at least 10% the thrust force. Values $E = 5 \times 10^{10}$ Pa and $\nu = 0.29$ have been used in the calculations [9].

(This figure is in colour only in the electronic version)

where the bending moments M_x, M_y are

$$M_x = \int_{-h/2}^{h/2} \tau_{xx} z \, \mathrm{d}z = -D \left[\nu \frac{\partial^2 w(x, y)}{\partial y^2} + \frac{\partial^2 w(x, y)}{\partial x^2} \right], \quad (7a)$$

$$M_y = \int_{-h/2}^{h/2} \tau_{yy} z \, \mathrm{d}z = -D \left[\frac{\partial^2 w(x, y)}{\partial y^2} + \nu \frac{\partial^2 w(x, y)}{\partial x^2} \right], \quad (7b)$$

whereas shear stresses are comparatively negligible.

It can be conjectured that if the two consecutive septa are approximately parallel as in *Manticoceras* (see figure 1), the above equation for the rectangular plate can be applied also for a curved plate. This can be justified heuristically thinking of a rectangular plate with one side much longer than the other. The displacement of the plate at some point is mainly determined by the shortest chord supported by the boundaries and passing through the point, which in a rectangular plate is simply the shorter side of the rectangle. This holds true also for a plate where the sides are curved and parallel as in figure 2, provided that the sides of the plate do not bend rapidly (the distance between the parallel sides has to be much smaller than the radius of curvature).

In this approximation, the length a has to be replaced by the length of the suture line Γ, whilst b is replaced by $ab/\Gamma = A/\Gamma$, so that the area of the plate A remains constant. Calculations have been reported in figure 3, where the two graphs show the maximum stress in the plate (*A*) and the total deformation Δ of the plate (*B*) as a function of the ratio $R = a/b$. The five curves for each graph have been obtained with different values for plate thickness and area $A = ab$ and for a pressure of 1 MPa corresponding to approximately 100 m of water depth. The chosen thicknesses are in the range of ammonoids and Nautili. Note that the wall thickness of ammonoids has been measured in a limited number of cases. For example, Hewitt and Westermann [2] report values between 0.07 mm (*Goniatites*) and 3 mm for the giant *Baculites*, whereas *Perisphinctes* (shown in figure 1) has a wall thickness of 0.31 mm (values referred to the last ontogenetic stages). In contrast, modern adult Nautili have wall thicknesses higher than 1 mm. Thus, to include in the analysis both ammonoids and Nautili, I have chosen thicknesses between a fraction of mm to some mm, as presented in figure 3.

From figures 3(*A*) and (*B*), one can appreciate that both the maximum stress and the total deformation Δ decrease dramatically as a function of the suture length. In particular, an increase by a factor of 3–4 in the ratio R entails a substantial reduction of plate deformation by about two orders of magnitude. It can be concluded that an increase in the length of a suture line in the model ammonoid results in a strong reduction of both the stress in the shell and in the shrinkage volume of a chamber. Note the dependence of both the stress and the deformation on the area of the plate. So,

Table 1. Data calculated for two different plates: A: $h = 0.5$ mm, $A = 6$ cm^2 (corresponding to green in figure 3) and B: $h = 0.5$ mm, $A = 10$ cm^2 (blue in figure 3). In the table, for both A and B, the data reported are the dimensionless suture length R defined as the ratio of the two plate lengths $R = a/b$, Δ defined in equation (6) at a depth of 100 m below the optimum depth, the shrinkage coefficient χ for the entire shell, the characteristic time τ and the force F consequent to buoyancy loss that a model ammonoid would experience at a depth of 100 m below the optimum level. The other parameters are $N_{\mathrm{cham}} = 10$, $M = 0.3$ Kg. Note that because calculations are performed at 1 MPa, and because the shrinkage coefficient χ has the units of cm^3 MPa^{-1}, the shrinkage volume δV for the entire shell is numerically equal to χ.

Relative length of suture R	Δ (cm^3)	δV (cm^3)	χ (cm^3 MPa^{-1})	$\tau(s)$ $M = 0.3$ Kg	$F(N)$ at $y - \bar{y} = 100$ m
			A		
2.66	0.286	5.72	5.72	22.86	0.057
10	0.028	0.56	0.56	73.1	0.0056
20	0.007	0.14	0.14	146.4	0.0014
			B		
2.66	1.373	27.46	27.46	10.39	0.274
10	0.132	2.64	2.64	33.8	0.026
15	0.061	1.22	1.22	49.5	6×10^{-4}

for example, a relatively large area of 10 cm^2 (red, blue and cyan) results in much higher stresses and deformations than a smaller area of 6 cm^2 (green and yellow). The result strongly depends also on the plate thickness. A thin plate wall of 0.5 mm (blue and green) is subjected—the other parameters being the same—to much higher stresses and deformations than a 1 mm thick plate (red and green) and a very thick one (cyan, 3 mm). Figure 3(A) also reports an estimated value (131 MPa) of the maximum tensile stress that nacre is capable to tolerate [4]. A shell with the properties as of the blue curve would have imploded for a ratio R less than about 7. However, more complex sutures (higher R) are capable of maintaining the maximum stress under the threshold value. For a sufficiently thick shell (see the example in cyan) the yield stress is never reached, a strategy used by modern Nautili (which, indeed, do not exhibit complex suture lines).

From figure 3(B), one can appreciate the effect of volume decrease Δ of a single plate. The volume decrease of the whole model ammonoid shell subject to the external pressure P is

$$\delta V = 2N_{\mathrm{eff}}(\partial\Delta/\partial P)P \equiv \chi P, \tag{8}$$

where N_{eff} is an effective number of chambers (assuming they all have the same properties) and the factor 2 derives from the presence of two faces for every chamber. The quantity $\chi = \delta V/P$ is a shrinkage coefficient giving the contraction of the entire shell in response to uniform pressure. Note that as long as we are in the elastic regime, stress and deformation will depend linearly on the pressure. In the following, I set $N_{\mathrm{eff}} = 10$. As an example, an ammonoid with the properties as of the red curve in figure 3 ($h = 1$ mm, $A = 10$ cm^2) would have been subjected to a deformation of about 5 cm^3 (for small R) and to a much smaller value of about 0.15 cm^3 for $R \approx 15$. Table 1 shows data for the two previous cases of figure 3 with an external wall area of $A = 6$ cm^2 and $A = 10$ cm^2, and shell thickness $h = 0.5$ mm corresponding to the green and blue cases respectively. The volume loss of the entire shell (third column in table 1) decreases markedly with an increasing relative suture length. The fourth column also reports the shrinkage coefficients for these cases.

It can be suggested that the deformation and shrinkage of a hypothetical 'badly built' ammonoid (i.e. having a thin shell, non-complex suture line and large chamber area exposed to external pressure) was not negligible, and such as to decrease significantly its buoyancy. The loss of buoyancy due to shell shrinkage would have been of the order $F = \delta V g\rho_w$ where g is gravity acceleration and ρ_w is water density. With a value of 5 cm^3, this corresponds to a force of about 0.05 N. Similar to Nautili, ammonoids were able to shift vertically by pumping water through the hyponome, generating a thrust force of the order

$$F_{\mathrm{thrust}} \approx \tfrac{1}{2}\rho U^2 S = P_{\mathrm{int}} S, \tag{9}$$

where U is the average velocity of the water jet, P_{int} is the internal pressure (in the mantle cavity) and S is the area of the hyponome opening. The value measured for squid [12] is $P_{\mathrm{int}} = 5300$ Pa (which corresponds to $U = 2.6$ m s^{-1}) and with $S \approx 0.1 - 0.5$ cm^2 (a value only guessed owing to lack of conservation of ammonoid soft parts) one gets a thrust force of the order $0.053 - 0.26$ N. Chamberlain [13] has reported a maximum thrust for living Nautili of the order 0.01 to 1.4 N, according to the size of the specimen. If the mollusk performs series of rhythmical jets to maintain a constant velocity, then the thrust averaged in time must be equal to the drag force. This implies that the useful thrust is diminished by the drag force, and falls to 0.015–0.12 N [13]. These values are of the order of the buoyancy loss that a 'badly built' ammonoid must have experienced. In figure 3(B), the dark shaded area corresponds to a loss of buoyancy at 100 m depth higher than the thrust force (assumed value of 0.05 N). Because the only known means for an ammonoid to shift vertically was through the water jet (the old analogy with the submarine according to which Nautili and ammonoids could fill and empty the camerae at will for such purpose is known today to be untenable [10]), an ammonoid with these characteristics would have been incapable of counteracting buoyancy loss. The effect of buoyancy loss was probably important also below such values because the mollusk would have used energy to readjust its position in the water column with the water jet. I tentatively assume that the mollusk fitness was negatively affected when the buoyancy loss was at least 10% of T_{max} (light shaded region in figure 3(*B*)). Looking at the example in green of figure 3(*B*), one can note that an increase of the suture length in the model ammonoid determines a gradual passage from conditions where the buoyancy loss would be superior to the thrust force to a situation where it is reduced to a negligible amount.

We now examine in more detail the possible consequences of buoyancy loss for an ammonoid. It can be assumed that the ammonoid shell is best suited for a certain depth $\bar{y}$ below sea level, at which level the mollusk would neither rise nor sink. Because of shell shrinkage, an ammonoid floating on a level above $\bar{y}$ would have experienced an increase in the chambers volume, causing it to rise even more, whereas an ammonoid below the optimum level would have sunk. This makes the depth $\bar{y}$ a level of unstable equilibrium. The excess deformation is proportional to the pressure difference between the equilibrium depth $\bar{y}$ and the actual depth of the ammonoid y (equation (8)). Neglecting frictional drag, the equation of motion for the depth y of the ammonoid as a function of time can be written as

$$M\frac{\mathrm{d}^2 y}{\mathrm{d}t^2} = \chi(P - \bar{P})\rho g = \chi\rho^2 g^2 (y - \bar{y}), \qquad (10)$$

which gives a solution

$$y(t) = (y_0 - \bar{y})\,\mathrm{e}^{t/\tau} + \bar{y} \qquad (11)$$

where y_0 is the initial depth of the ammonoid below the equilibrium depth ($y_0 > \bar{y}$, with y positive downwards), and

$$\tau = \frac{1}{\rho g}\left[\frac{M}{\chi}\right]^{1/2} \qquad (12)$$

is the characteristic time of sinking. The numerical value for τ can be estimated based on the previous calculations and on assumed masses for ammonoids. Looking back at table 1, the numerical examples based upon the previous case of figure 3 (with an external wall area of $A = 6$ cm^2 and $A = 10$ cm^2), one can see that the characteristic time τ of a model ammonoid with the above characteristics is very short for a straight line (for such short times, the corresponding velocities become so high that the drag force is no longer negligible). With a suture line of relative length 15–20, the time becomes of some minutes, showing that it would have been much easier in this case to compensate for buoyancy loss by jet propulsion.

Table 1 also shows in the sixth column that for a suture line of 6 cm in length, the force at a depth of 100 m below the optimum level is about 0.04 N, while it becomes about 0.0008 N for a suture line of length 18 cm. This force is comparable to the force arising from buoyancy loss at 100 m deviation from the optimum level for the model ammonoid (see table 1) for the case with a short suture length. Instead, an ammonoid with a longer suture length would have experienced a much smaller buoyancy loss. Although this calculation is affected by major uncertainties, it points to the basic problem that an ammonoid with straight suture lines would have needed to correct its level frequently with a powerful water jet. Not only, as remarked earlier, would this behaviour have caused a substantial energy loss, but it is also at variance with the observations of living Nautili, which are slow swimmers and use jet propulsion only occasionally to escape predators. Additionally, a badly built ammonoid might have hypothetically reached a fatal non-return point if buoyancy loss was greater than the maximum thrust force attainable.

Also note that because the external shells of ammonoids were usually thin compared to modern Nautili (typically a fraction of mm compared to several mm), and because both stress and buoyancy loss increase markedly with decreasing thickness ($\tau \propto h^{-2}$, $\Delta \propto h^{-3}$), high stress and shell shrinkage must have been a more severe problem for ammonoids than it is for living Nautili. Thus, because of the greater thickness of the phragmocone wall in Nautili, the measurements of strain in the septa of living Nautili subjected to increasing pressure (see [14] and the experimental papers cited therein) are probably not directly applicable to ammonoids. Additionally, Nautili have a higher shell curvature than most ammonoids which, with the drawback of an increased drag, also contributes to mechanical robustness. Increasing the thickness of the shell was an evolutionary strategy requiring a greater effort for the production of nacreous shell, which would have also become more massive. Rather, ammonoids evolved towards augmenting the support of the external shell by surrounding the plate with a longer perimeter, which probably required a lower rate of nacre production.

Conclusions

Calculations illustrate the role of suture length in diminishing the stress and of deformation in ammonoid phragmocones, a conclusion valid also for more complex geometries where finite element methods must be applied [15]. Whereas the effect of stress decrease with increasing suture length confirms previous investigations [5], shell shrinkage and the ensuing loss of buoyancy is a newly suggested mechanism. Probably complex suture lines reduced both the stress and shell shrinkage caused by hydrostatic pressure, with the effect of improving buoyancy and dynamical stability of ammonoids through the water column, also at pressures lower than the point of catastrophic implosion. Note that deformation of nacreous plates of the order of the one calculated here is commonly measured in the laboratory [16]. Although calculations are applicable to the simplest suture lines of the most primitive ammonoids, the evolutionary biology of ammonoids demonstrates certain continuity in complexity increase over geological time, and thus it seems likely that an explanation valid for the simplest suture lines may hold also for the complex ones.

Even considering the simplest suture lines, the present estimates are greatly simplified compared to the real geometry of ammonoids. Firstly, the curvature of the phragmocone, the uneven wall thickness and the external ornamentation, not considered in the present work, certainly contributed in reducing both stress and deformation. Secondly, the nacre microstructure and its orientation with respect to principal stresses were almost certainly devised to gain an optimal performance, and the usage of an average value necessarily introduces a strong simplification. Finally, chambers have different properties depending on their ontogenetic stage.

Clearly, more complete calculations should be attempted to assess the role of suture complexity in diminishing stress and deformation in ammonoid phragmocones.

It is interesting to note that buoyancy loss resulting from pressure shrinkage is the same reason why submarine hulls are constructed with thick metal and not with materials of low Young's modulus such as glass fibres, which would otherwise represent an attractive alternative (see, for example, Gordon [17] for a popular account). Addressing the problem of ammonoid suture lines may have potential applications to the engineering of hollow structures subjected to high pressures such as submersibles and submarines.

References

[1] Clarkson E N K 1998 *Invertebrate Palaeontology and Evolution* 4th edition (Oxford: Blackwell)
[2] Hewitt R A and Westermann G E G 1986a *N. Jb. Geol. Palaont. Abh.* **172** 47–69
Hewitt R A and Westermann G E G 1986b *N. Jb. Geol. Palaont. Abh.* **174** 135–69
[3] Perez-Claros J A, Palmqvist P and Oloriz F 2002 *Math. Geol.* **34** 323–41
[4] Buckland W 1836 *Geology and Mineralogy Considered with Reference to Natural Theology* vols. 1, 599 (London: Pickering) pp 128
Pfaff E 1911 *Jahreshefte des Niedersachsischen Geologischen Vereins* **4** 207–23
[5] Hewitt R A and Westermann G E G 1997 *Lethaia* **30** 205–12
[6] Henderson R 1984 *Palaeontology* **27** 461–8
Lewy Z 2002 *Z. J. Paleont.* **76** 63–9
[7] Hammer Ø 1999 *Hist. Biol.* **13** 153–71
Checa A G and Garcia Ruiz J M 1996 *Ammonoid Paleobiology* ed N H Landman, K Tanabe and R Arnold Davis (New York: Plenum)
[8] Daniel T L, Helmut B S, Saunders W B and Ward P D 1997 *Paleobiology* **23** 470–81
[9] Hassan M A, Westermann G E G, Hewitt R A and Dokainish M A 2002 *Paleobiology* **28** 113–26
[10] Ward P D 1982 *Paleobiology* **8** 426–33
[11] Solecki R and Conant R J 2003 *Advanced Mechanics of Materials* (New York: Oxford University Press)) p 764
[12] Webber D M and O'Dor R K 1986 *J. Exp. Biol.* **126** 205–24
[13] Chamberlain J A 1987 *Nautilus: The Biology and Paleobiology of a Living Fossil* ed W B Saunders and N H Landman (New York: Plenum) pp 489–525
[14] Hewitt R A and Westermann G E G 1987 *Nautilus: The Biology and Paleobiology of a Living Fossil* ed W B Saunders and N H Landman (New York: Plenum) pp 435–61
[15] De Blasio F 2006 *Lethaia* submitted
[16] Wang R Z, Suo Z, Evans A G, Yao N and Aksay I A 2001 *J. Mater. Res.* **16** 2485–93
[17] Gordon J E 1976 *The New Science of Strong Materials* (Harmonsworth: Penguin Books)